ChemPubSoc Europe

DOI: 10.1002/open.201900336

Open Access ChemistryOPEN Reviews

Special Collection

Semiconductor Quantum Dots as Components of Photoactive Supramolecular Architectures

Marcello La Rosa,[a, b] Emily H. Payne,[a, c] and Alberto Credi*[a, d]

Dedicated to Professor Jean-Marie Lehn on his 80th birthday

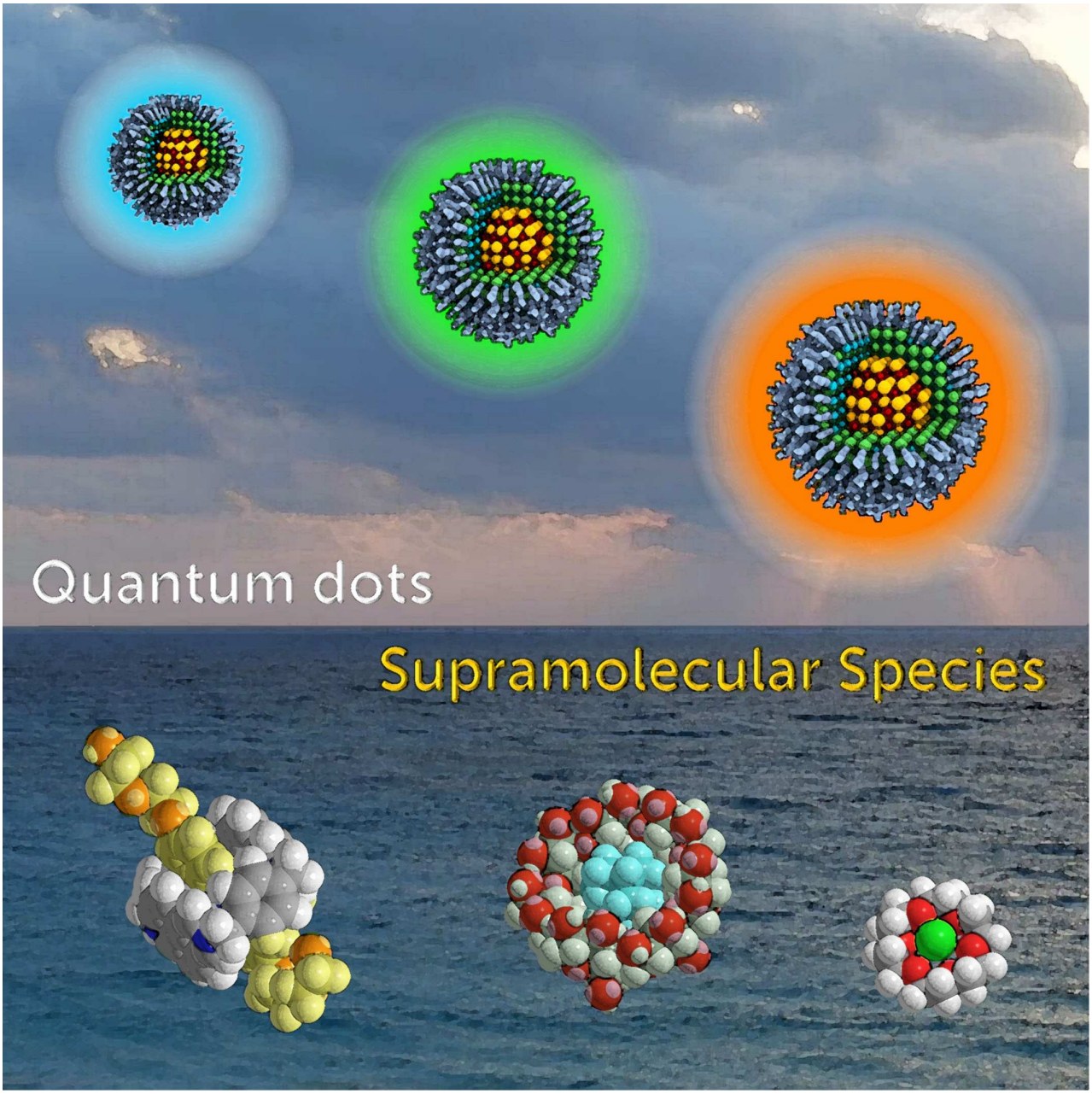

Luminescent quantum dots (QDs) are colloidal semiconductor nanocrystals consisting of an inorganic core covered by a molecular layer of organic surfactants. Although QDs have been known for more than thirty years, they are still attracting the interest of researchers because of their unique size-tunable optical and electrical properties arising from quantum confinement. Moreover, the controlled decoration of the QD surface with suitable molecular species enables the rational design of inorganic-organic multicomponent architectures that can show a vast array of functionalities. This minireview highlights the recent progress in the use of surface-modified QDs – in particular, those based on cadmium chalcogenides – as supramolecular platforms for light-related applications such as optical sensing, triplet photosensitization, photocatalysis and phototherapy.

1. Introduction

Luminescent semiconductor nanocrystals, or quantum dots (herein referred to as QDs), are of great interest due to their unique and highly useful photophysical properties, such as a broad-band absorption spectrum with very large molar absorption coefficients, relatively long luminescence lifetimes, high photoluminescence quantum yields and superior photostability.[1,2] Owing to their size, typically ranging between 1 and 10 nm, QDs are strongly affected by quantum confinement effects, which ultimately make their optical and electronic properties size dependent.

Research in the field of semiconductor QDs started in the early 1980s, when Ekimov[3] and Brus[4] reported the formation of nanoscale-sized crystals in glassy matrix and colloidal solutions, respectively. In the beginning, QDs were mainly fabricated and studied for quantum mechanics investigations. However, as soon as efficient and reliable synthetic protocols providing high-quality luminescent nanocrystals became available,[5] QDs have started to attract the attention of researchers from several disciplines, including chemistry, physics, biology, materials science and engineering. The increasing interest on these nanomaterials is witnessed by the impressive number of papers,[6] reviews[7] and books[8] published in the past two decades.

Today, after more than thirty years since their discovery, the knowledge of such systems has significantly expanded from the fundamental understanding of the quantum mechanical properties[9] to the development of QD-based technologies for the mass-market.[10] Quantum dots are now recognized as emerging materials for practical applications ranging from catalysis to sensing, and from nanomedicine to photovoltaics. Indeed, several manufacturers, including Samsung, LG, and Sony, are now offering consumer electronic devices (from mobile phones to large screen tv) endowed with quantum dot-containing displays.

It should be pointed out that a detailed understanding of the properties of the nanocrystal surface is essential for designing any QD-based material or device.[11] In fact, because of the small size of the nanocrystals, surface properties and processes can deeply affect the physical and chemical behaviour of the QDs. As it will be discussed in the next sections, molecular species that can bind to the nanoparticle surface (often referred to as surfactants or capping ligands) are a fundamental ingredient in the preparation, processing, investigation and exploitation of QDs. Furthermore, surface ligands can be endowed with active moieties (for example, photo- or redox-responsive units, receptors, catalytic sites, etc.), with the purpose of implementing functionalities that could arise from the interplay between the QD and molecular components (Figure 1).[12,13]

As the field has progressed, attention has been spread to a wide variety of semiconductor nanoparticles that experience quantum confinement effects,[7,8] such as perovskite nanoparticles[14,15] and other QDs made of non-toxic and earth-abundant elements.[16] An intense research effort, however, is still focused on cadmium chalcogenides (typically, CdS, CdSe and CdTe), despite the potential toxicity[17] and environmental issues associated with Cd-based compounds.[7g,18] This is mainly

[a] Dr. M. La Rosa, E. H. Payne, Prof. Dr. A. Credi
CLAN-Center for Light Activated Nanostructures
Istituto per la Sintesi Organica e la Fotoreattività, Consiglio Nazionale delle Ricerche, Via Gobetti 101, 40129 Bologna, Italy
E-mail: alberto.credi@unibo.it
[b] Dr. M. La Rosa
Dipartimento di Scienze e Tecnologie Agro-alimentari
Università di Bologna, Viale Fanin 50, 40127 Bologna, Italy
[c] E. H. Payne
EaStChem School of Chemistry, The University of Edinburgh
David Brewster Road, Edinburgh EH9 3FJ, UK
[d] Prof. Dr. A. Credi
Dipartimento di Chimica Industriale "Toso Montanari"
Università di Bologna, Viale Risorgimento 4, 40136 Bologna, Italy

An invited contribution to a Special Collection dedicated to Functional Supramolecular Systems

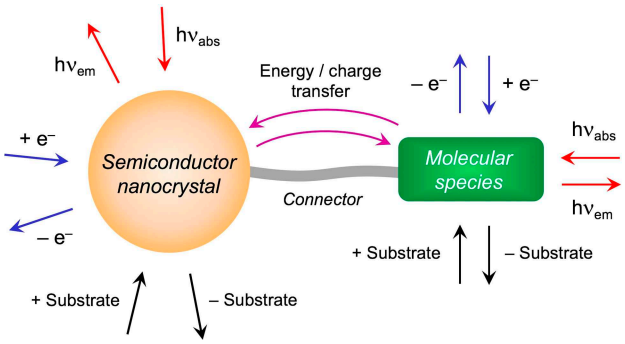

Figure 1. Schematic representation of a nanohybrid consisting of QD and molecular components, and of the processes that can take place within the hybrid and with external species. The different components are not on the same scale.

because their band gap energy enables the fine tuning of the QD absorption and emission features across all the near-UV, visible and near-IR regions. Indeed, it is with these well-known materials that major leaps towards a detailed fundamental understanding and advanced applications continue to be made.

The aim of this minireview is to provide an overview on functional supramolecular devices that comprise cadmium chalchogenide QDs as photoresponsive components. After an introduction on the physical and chemical properties of this kind of nanocrystals, a few recent examples of QD-based nanodevices capable of performing light-activated tasks, such as optical sensing, triplet sensitization, catalysis and drug delivery, will be briefly described.

1.1. Basic Physical and Chemical Properties of QDs

The energy gap (E_g) between the valence and the conduction bands is a distinctive property of any material. Upon absorption of a photon with suitable frequency ($h\nu \geq E_g$), one electron (e^-) may be promoted from valence to conduction levels, thus leaving a hole (h^+) in the valence band (Figure 2a). The resulting pair of charge carriers is called an exciton, and the average separation between the charges of the exciton is known as the Bohr radius. For example the Bohr radius of CdSe is 5.6 nm.[19]

The band gap energy of a bulk material is determined exclusively by the electronic structure of the compound, which in turn depends on its chemical composition. However, if the size of a semiconductor fragment approaches the Bohr radius, the electron and hole wavefunctions become spatially confined. Nanoparticles that experience such a quantum-confined regime are referred to as quantum dots (Figure 2b).

Within a simple approximation, the quantum mechanical properties of QDs can be described in terms of a "three-dimensional box" where the exciton is confined.[9b] According to this model, the resulting electronic configuration exhibits discrete energy levels within both the valence and the conduction bands. The E_g value is directly proportional to $1/R^2$, where R is the QD radius; in other words, the smaller the size of the nanocrystals, the higher the band gap (Figure 2b).

The absorption spectrum of QDs (Figure 3) is characterized by a sharp band on the low energy side, corresponding to population of the first exciton state exhibiting a strong oscillator strength (the so-called bright state). For the reasons described above, the maximum wavelength and intensity of this band depend on the particle size.[20] Unlike typical molecular dyes, that possess discrete absorption bands (Figure 3), QDs exhibit quite large molar absorption coefficients (in the range between 10^4 to 10^6 $M^{-1}cm^{-1}$) over a broad spectral region, thus enabling effective excitation on a wider range of wavelengths and with lower light intensities than molecular dyes.[2,21]

The decay of the exciton (i.e., the recombination of the charges) can occur radiatively and cause the emission of a photon (Figure 2). This process has a very high probability for direct band gap semiconductors (i.e., in which the lowest

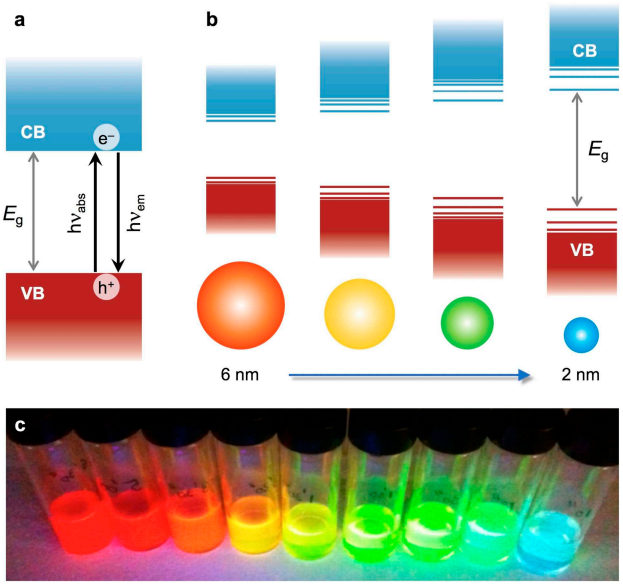

Figure 2. (a) Diagram showing the valence (VB) and conduction (CB) bands of a semiconductor, and representation of the photoinduced generation of an exciton and its radiative recombination. (b) Effect of quantum confinement on the electronic configuration of semiconductor nanocrystals. (c) Photographs showing the luminescence arising from colloidal solutions of CdSe QDs of different size, excited with UV light.

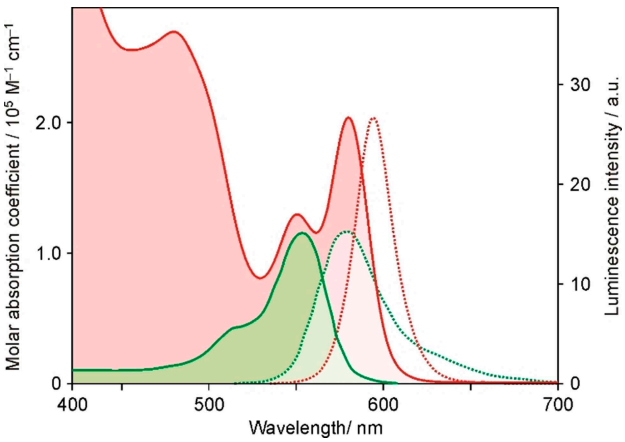

Figure 3. Absorption (full line) and luminescence (dotted line; $\lambda_{exc} = 500$ nm) spectra of CdSe QDs (red traces; $R = 1.9$ nm, chloroform) and of a popular dye such as Rhodamine B (green traces, methanol) at room temperature.

Alberto Credi is professor of Chemistry at the University of Bologna and director of the Center for Light Activated Nanostructures (CLAN), a University-National Research Council joint laboratory for research in photochemistry, supramolecular chemistry, materials science and nanoscience. He has coauthored 4 books and over 280 scientific publications, and he is the PI of an ERC Advanced Grant for the development of light driven molecular motors.

energy conduction level and the highest energy valence level have the same momentum) like cadmium chalcogenides, leading to theoretical emission quantum efficiencies close to unity.

The emission band is sharp and Gaussian-shaped, in contrast to the broader and red-tailored spectral profile exhibited by molecular fluorophores (Figure 3). It is worth noting that the shape of such an emission band is also related to the size distribution of the nanocrystal population. Indeed, for a highly monodisperse sample the emission fwhm (full width at half maximum) is typically lower than 30 nm; larger values of this parameter indicate a broad size distribution. It is evident that the ability to prepare monodisperse samples with controlled radius and high purity[22] is crucial in order to take full advantage of the size-dependent optical properties of QDs.

In summary, the absorption and emission energies of QDs can be finely tuned from the UV to the IR region by playing with the chemical composition to select the band gap of the bulk material, and with the size of the particles to exploit quantum confinement (Figure 2c). Other aspects in which QDs outperform molecular dyes are the two-photon absorption properties and the photochemical stability. For all these reasons, semiconductor nanocrystals are appealing candidates for applications that involve irradiation at high intensity for long times,[23] or single-particle detection.[9a,24]

The luminescence, however, can be prevented by recombination of the exciton via non-radiative processes. These phenomena are related to the presence of intra-band gap energy levels that arise from surface "dangling bonds" and/or local defects in the crystal lattice. Thus, an efficient passivation of the surface is an essential requirement to obtain highly emissive QDs. As it will be discussed in the next section, this goal can be achieved by an appropriate choice of the capping ligands.

Another strategy consists of coating the nanocrystals with an overlay of another semiconductor material having a larger bandgap (core-shell nanocrystals, type I).[7c] The most popular case is that of CdSe–ZnS core-shell QDs,[25] which are commercially available in various sizes. Due to the band gap difference between the core and the shell, the exciton is confined within the core and recombines through the corresponding band edges; as a consequence, the properties of the resulting nanocrystals are qualitatively determined by the size and composition of the core, but are significantly enhanced by the presence of the shell.

As it can be imagined, the combination of different semiconductor materials can give access to a virtually huge library of core-shell nanocrystals. QDs with tailor made properties may be obtained by engineering the band gaps at the interface between different materials; interested readers can refer to specific literature.[7c,25,26]

1.2. The Importance of the Surface

Taming the reactivity of the nanocrystal surface is key to control the synthesis, colloidal stability, solubility, opto-electronic properties and chemical behaviour of QDs. This task is performed by the molecular surfactants. Although a full understanding of the interactions that occur at the nanocrystal surface requires several concepts from surface and coordination chemistry,[11,27] the binding of the capping ligands can be described in similar terms as for metal complexes.[28] According to this model, three main groups of capping ligands can be identified, depending on the number of electrons involved and the electron donor or acceptor nature of the ligands:[29]

- L-type: neutral electron pair donors interacting with the metal component of the nanocrystal surface. Archetypes of such ligands are amines, phosphines and phosphine oxides.
- X-type: monovalent anions (e.g., carboxylates, thiolates and phosphonates) that coordinate electron poor sites at the nanocrystal surface.
- Z-type: Lewis acids interacting with electron rich sites at the nanocrystal surface. Examples are $Pb(OOCR)_2$ and $CdCl_2$.

As anticipated above, the photophysical properties are affected by the number of surface traps, which in turn depend on the passivation provided by the capping ligands.[30] Indeed, CdSe QDs coated by linear L-type ligands such as primary amines with long aliphatic chains showed a stronger emission (quantum yields up to 60%) than those coated by more sterically hindered *n*-alkylphosphine oxide L-type ligands.[31] Recently, the incorporation of X-type ligands, such as chloride anions, during the synthesis of PbS[32] and CdS[33] QDs was found to afford an efficient passivation of the surface trap sites, impossible to achieve with larger organic ligands. The ability of Z-type ligands to fully saturate the anionic surface trap states in QDs made of II–VI and III–V semiconductors was also reported.[34]

Although significant progress has been made in the aqueous phase synthesis of hydrophilic nanocrystals,[35] most synthetic routes that offer an excellent size and shape control of QDs involve the reaction of inorganic precursors in apolar or amphiphilic organic solvents, in the presence of the capping ligands.[8] These methods yield highly hydrophobic QDs, soluble only in apolar organic solvents such as toluene, hexane or chloroform, whose surface is typically coated with tris(*n*-octyl) phosphine oxide (TOPO, see Figure 4), alkylamine and/or alkanethiol ligands.[36] An important aspect of most surfactants is the dynamic nature of their binding to the nanoparticle surface, which allows the exchange of the native ligands with other molecules bearing different functionalities (Figure 4a).[36,37] For example, biological uses require that the QD surface be engineered in order that the particle is soluble in water.[7d] Of course, QDs functionalized with molecular units that are soluble in organic solvents can also be prepared by ligand exchange procedures.

Lipoic acid-based species have proven to be particularly suitable to obtain stable QDs by ligand exchange.[37a] Lipoic acid consists of a 1,2-dithiolane moiety, which can act as a bidentate surface binding group, connected by means of a short alkyl chain to a carboxylic end group, that can confer water solubility or be further functionalized (Figure 4a).[38] Versatile methods for the chemical[39] or photochemical[40] activation of 1,2-dithiolane

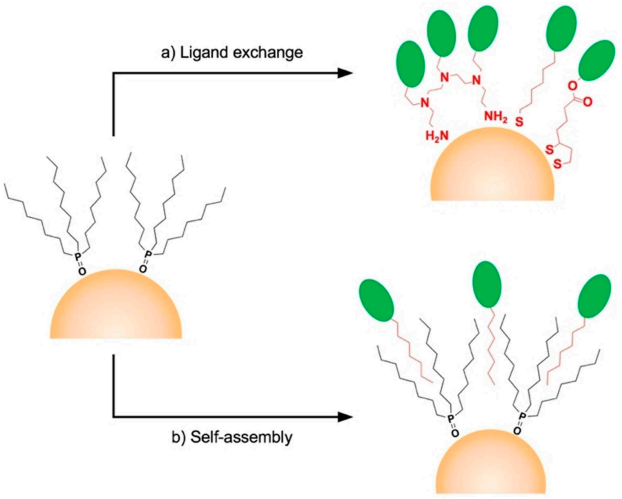

Figure 4. Strategies for the surface modification of natively hydrophobic QDs coated by tris(*n*-octyl)phosphine oxide. (a) Ligand exchange with amine-, thiol- or 1,2-dithiolane-type molecules. (b) Self-assembly of the nanocrystal capping layer with molecules endowed with a long alkyl chain, driven by Van der Waals interactions. The green ovals represent functional units.

derivatives to replace the native surface ligands of QDs have been recently reported.

The complexation of appropriate molecular species by the monolayer of the capping ligands (Figure 4b) offers an alternative approach to modify the chemical nature of the nanocrystals surface. Such a route requires neither the synthesis of derivatives in which the molecule of interest is connected to a docking moiety for the QD surface, nor the optimization of ligand exchange procedures. On the other hand, the surface capping ligands and the functional species to be associated with the QDs need to possess molecular recognition elements to promote an efficient self-assembly under given conditions. To this aim, one can take advantage of a variety of intermolecular interactions, that includes hydrogen bonding, solvophobic effects, Van der Waals forces and electron donor/acceptor interactions.

A straightforward possibility in this sense is provided by the encapsulation of the nanocrystals into oil-in-water micelles. This process is first driven by the interactions between the hydrophobic tails of suitable amphiphilic molecules and those of the surface capping ligands; then, the hydrophilic outer heads of the amphiphiles ultimately provide water solubility to the resulting embedded nanocrystals. For example, phospholipids,[41] organoammonium ions[42] and amphiphilic polymers[43] have been employed for transferring nanocrystals into such micelles. Nevertheless, drawbacks such as the detachment of the molecular coating, degradation of the optical properties and nanocrystals aggregation, limit the versatility of such an approach, particularly in biological conditions.

Alternatively, ligand exchange procedures can be applied to coat the QD surface with ligands bearing specific molecular hosts or guests subunits. In recent times, for example, semiconductor nanocrystals functionalized with well known macrocyclic hosts in supramolecular chemistry – crown ethers,[44] cyclodextrins,[45] calixarenes,[46] and cucurbiturils[47] – have been reported, and their association with suitable molecular guests has been investigated, usually for sensing purposes.

2. Luminescent Chemosensors

The photophysical properties of pristine (i.e. as-synthesized) quantum dots are generally not affected by the presence of molecular or ionic species in the surrounding medium. This is particularly true for strongly emissive nanocrystals, which are those that can potentially ensure high sensitivity in luminescent measurements. In fact, QDs that possess large emission quantum yield are characterized by a very efficient passivation of their surface (by an inorganic coating and/or the monolayer of capping ligands), thus rendering them inherently insensitive to the surrounding environment. Hence, strategies to obtain a luminescence sensing response with QDs typically involve their conjugation with chemosensitive molecular components.[48] In some cases, however, the surface passivating ligands may also act as receptors to certain analytes, or 'direct' the analyte to the surface of the nanocrystal, thus favouring interactions or chemical reactions between them.

As depicted in Figure 5, a common design of luminescent chemosensors comprises three components: a luminophore (L); a quencher (Q) able to prevent the emission of L by means of specific mechanisms; and a control component (R) that affects the quenching ability of Q, as a consequence of the binding of the analyte A. Frequently, the roles of Q and R are played by the same component. Chemosensors based on the enhancement of the luminescence intensity of L upon analyte binding are referred to as 'turn-on' sensors (see, e.g., Figure 5). Conversely, in 'turn-off' sensors the recognition of the analyte causes a quenching of the luminescence of L.

Clearly, in the present context we focus on sensors in which the L component is a luminescent QD. The modulation of the luminescence response in these systems can be achieved by exploiting photoinduced electron- or energy-transfer processes. An electron transfer from a photoexcited QD to a surface-bound electron acceptor (A) can occur if the LUMO of the latter lies at a lower energy than that of the edge of the conduction band (Figure 6a). On the other hand, if the HOMO of a surface-bound electron donor (D) is higher in energy than the edge of the valence band, the electron transfer can occur in the reverse

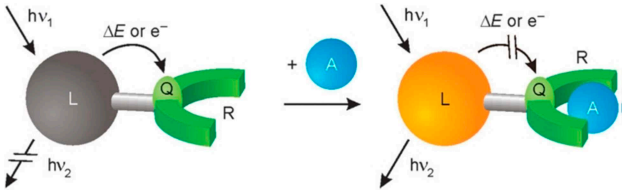

Figure 5. Scheme of the analyte-modulated 'turn on' photoluminescence response in a luminophore-quencher-receptor multicomponent chemosensor. Reproduced with permission from Ref. [48d]. Copyright 2015 Royal Society of Chemistry.

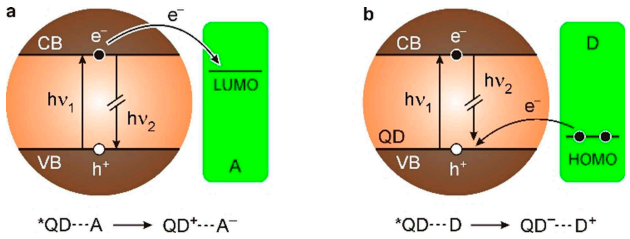

Figure 6. a) Schematization of an electron transfer from a photoexcited QD to an electron acceptor A, and b) an electron transfer from an electron donor D to a photoexcited QD. Adapted with permission from Ref. [48d]. Copyright 2015 Royal Society of Chemistry.

direction (Figure 6b). In both cases, the exciton recombines non-radiatively and the luminescence of the QD is quenched.

Another important photoinduced process that can take place in a QD-molecule conjugate is Förster-type (or dipole-dipole) resonance energy transfer (FRET). The majority of QD-based chemosensors show FRET from the nanocrystal to the surface-bound chromophore (Figure 7a). Electronic energy transfer in the opposite direction is less common for spectroscopic reasons:[50] as discussed in Section 1.1, QDs exhibit a broad and intense UV-visible absorption spectrum, and therefore their photosensitization while avoiding direct excitation is quite challenging.

Although a detailed discussion of energy- and electron-transfer mechanisms is beyond the scope of this work and interested readers can refer to specific references,[13,49,50] it is worth mentioning that several parameters such as the distance between the donor and the acceptor, the electronic coupling and the individual spin properties have to be rationally considered in the design of any luminescent supramolecular chemosensor. Indeed, if the presence of a target analyte affects

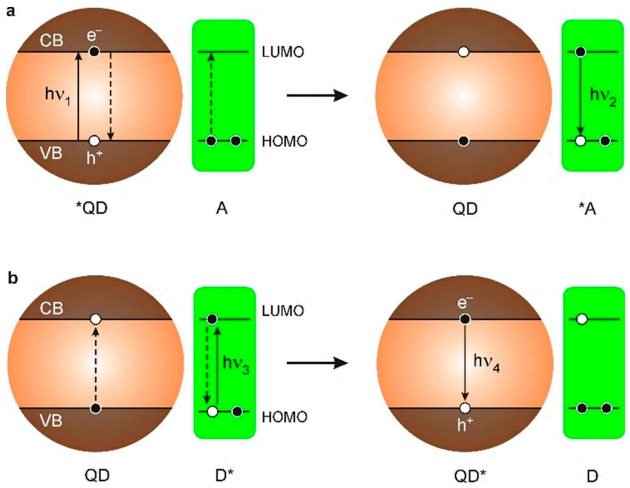

Figure 7. Schematization of Förster resonance energy transfer (FRET): a) from a photoexcited QD to a molecular energy acceptor (A); b) from a photoexcited molecular energy donor (D) to a QD. The energy-transfer process may give rise to photosensitized emission of the energy acceptor component ($h\nu_2$ for a, $h\nu_4$ for b). Adapted with permission from Ref. [48d]. Copyright 2015 Royal Society of Chemistry.

at least one of these parameters, then an optical sensing task can be performed.

Several examples of sensing of small molecules, biomolecules and anions carried out by inorganic-organic nanohybrids have been reported.[48,50,51] Here we focus on recent progress in metal ion sensing, ratiometric sensing, and improvement of sensitivity and detection limits.

2.1. Sensors For Metal Ions

CdTe QDs functionalized with ligands consisting of a 1,10-phenanthroline moiety covalently linked to two azacrown ethers were used for the optical sensing of metal ions based on photoinduced electron transfer (Figure 8).[52] Upon replacement of the native surfactants of the nanocrystal with the phenanthroline-azacrown ether ligands, the QD luminescence is quenched because of a photoinduced electron transfer from the phenanthroline HOMO. The addition of Ba^{2+} ions, which are complexed by the azacrown ether units, lowers the energy of the HOMO level, thereby making the oxidation of the phenanthroline moiety more difficult. Consequently, the electron-transfer quenching is prevented and the QD emission is strongly enhanced, thereby providing the basis for 'turn on' luminescent sensing of barium ions in organic solvent.

Metal ions can also interact with semiconductor nanocrystals via either direct incorporation into the surface or binding to the capping ligands.[53] It is worth noting that specific ion-mediated radiationless exciton recombination pathways, as well as ion binding interactions that lead to a less efficient surface passivation or agglomeration of nanocrystals, may also be responsible for the luminescence quenching. On the other hand, the formation of ion-ligand complexes at the surface could also restrict the conformational freedom of the ligands in such a way that a more ordered and/or rigid arrangement is achieved. As a consequence, the protection of the nanocrystal from the surrounding environment may be improved, resulting in an increase of the QD luminescence intensity. Nonetheless, surface defects and dangling bonds can be passivated by the incorporated ions.[53]

Significant effort has been dedicated to the optimization of both detection limit and selectivity of QD-based metal ion sensors.[54] The detection of traces (i.e., very low concentrations) of metal ions, particularly those of physiological relevance and marked toxicity, in samples such as water sources and biological

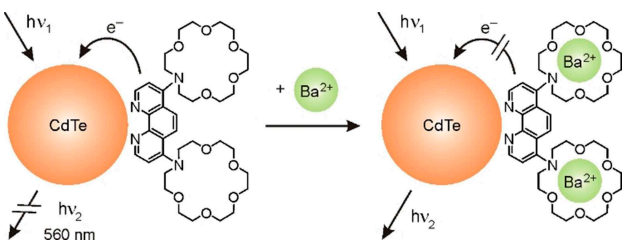

Figure 8. CdTe QDs functionalized with phenanthroline-azacrown ether ligands and scheme for the luminescent sensing of Ba^{2+} ions.[52]

matrices is indeed a highly important task. In an early work, Rosenzweig and coworkers[55] reported the switching of the luminescence response of water-soluble CdS QDs to certain metal ions, simply by changing the nature of surface capping ligands. In particular, polyphosphate-capped QDs were found to be sensitive to almost all mono- and bi-valent cations, showing no selectivity. On the other hand, thioglycerol-capped QDs showed a response only for Cu^{2+} and Fe^{2+} ions, whereas L-cysteine-capped QDs were sensitive to Zn^{2+} ions and insensitive to, e.g., copper, calcium, and magnesium ions.

Inspired by these results, Solanki and coworkers[56] recently developed two different CdSe QDs-based nanoprobes exhibiting significant selectivity for either Cu^{2+} or Zn^{2+} ions, depending on the surface ligands. CdSe QDs capped with 3-mercaptopropionic acid were found to be selective for Cu^{2+}, while those coated with L-cysteine showed selectivity for Zn^{2+} ions. Interestingly, such selectivity is expressed towards several physiologically important ions such as Fe^{2+}, Mg^{2+}, Pb^{2+}, Ni^{2+}, Co^{2+} and Ag^{+}. The detection limit of the two probes was comprised between 4 and 160 μM.

The two nanohybrids also exhibited different behavior in the ion recognition process. Specifically, the Zn^{2+} ions were found to enhance the photoluminescence of the cysteine-capped QDs. Such a response is mostly due to the complexation between the metal ions and the carboxylic moieties of L-cysteine ligands, which results in a more rigid conformational arrangement of the surface ligands. Conversely, the addition of Cu^{2+} ions to mercaptopropionic acid-capped CdSe QDs caused a quenching of the luminescence. Such an effect can be interpreted in terms of a photoinduced electron transfer from the QD to the metal ion. Additionally, Cu^{2+} ions are able to replace the native Cd^{2+} ions, thus forming poorly soluble particles of CuSe onto the surface. Charge transfer from the CdSe QDs to the CuSe particles was found to be much faster than the radiative exciton recombination, therefore causing the QD luminescence quenching.

Bardajee and coworkers[57] described a CdTe QD-based nanoprobe for the detection of Cu^{2+} ions in environmental water samples, featuring a sensitivity 10^2-fold greater than that of a previously reported analogous system.[58]

Despite the significant progress made in the area of QD-based luminescent probes for metal ions, what is still lacking is a rational design of the recognition process to be ion-selective. A recently reported strategy may provide insightful hints in this regard. Halder and coworkers[59] developed a nanoprobe, consisting of thiolactic acid-capped CdTe QDs, that exhibits an unprecedented selectivity for Ag^{+} ions.

In general, transition metal ions added to an aqueous solution of mercapto acid-capped QDs can undergo either adsorption on the QD surface (aided by the interaction with the soft sulfur atom) or coordination to the hard oxygen atom of the terminal carboxylate group.[59] However, in case of thiolactic acid as capping ligand, the surface adsorption process is the preferred one. This behaviour is ascribed to the fact that the methyl substituent adjacent to the carboxylate moiety makes the ion binding to the latter significantly unfavourable (Figure 9). The steric hindrance exerted by the methyl group is, therefore, responsible for the inhibited recognition of metal ions such as Zn^{2+}, Cu^{2+}, Pb^{2+} and Ni^{2+}. A similar effect was previously observed in the case of CdTe QDs capped with 3-mercaptobutyric acid.[60]

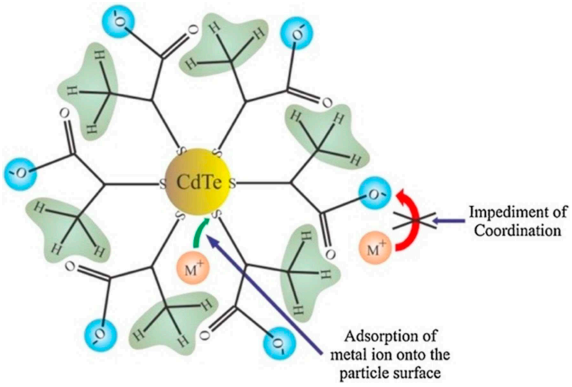

Figure 9. Schematic representation of the selective sensing mechanism of TLA-capped CdTe QDs toward metal ion detection. Adapted with permission from Ref. [59]. Copyright 2017 Elsevier.

Earlier literature reports[61] revealed that Ag^{+} ions quench the photoluminescence of QDs by either interacting with surface trap-states or causing the formation of silver chalcogenides on the surface that behave as electron/hole scavengers. Understanding the relationship between the structural properties of surface ligands (e.g., conformation, rigidity, and steric hindrance) and the sensing performance is the key for the design of QD-based probes with predetermined and selective analytical response.

2.2. QD-Based Ratiometric Sensors

In ratiometric luminescent sensing, the analytical signal is the ratio between the emission intensity measured at two different wavelengths on the same system, instead of a single emission intensity measurement. The advantage of the ratiometric response is that, being a relative quantity, it is independent on the instrumental setup, and its calibration is much simpler than that of an absolute signal. Thus, ratiometric optical sensors are highly desirable tools in analytical sciences.

Core-shell CdSe–ZnS QDs decorated with pyrenyl-terminated ligands (Figure 10) were employed to perform the ratiometric sensing of oxygen in organic solvents.[62] Oxygen is indeed a relevant analyte in a variety of applications, ranging from life sciences to environmental and food control. In this QD-pyrene conjugate the two luminophores are not interacting and behave independently from one another; hence, the emission spectrum shows the bands of both the pyrene (λ_{em} = 378 nm) and QD (λ_{em} = 632 nm) components. The luminescence properties of the nanohybrid are influenced by the presence of dissolved oxygen, because the surface-bound fluorophore is strongly quenched by O_2, whereas the QD emission is not (Figure 10b). Therefore, the QD emission intensity can be taken as an internal reference for the oxygen-dependent pyrenyl

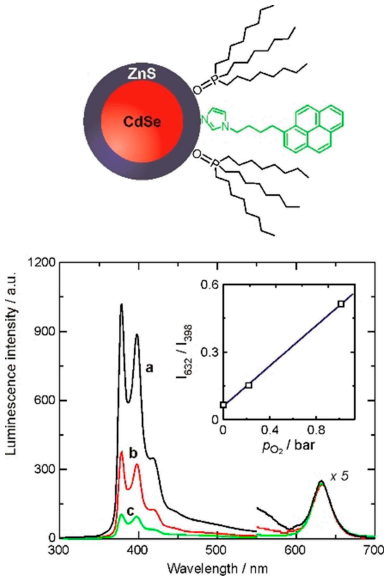

Figure 10. Luminescence spectra of CdSe–ZnS QDs functionalized with imidazole-pyrenyl ligands (schematically shown in the top part) in chloroform at room temperature as a function of the oxygen pressure: 0 (a), 0.213 (b) and 1.013 (c) bar (λ_{exc} = 275 nm). The inset shows the linear correlation between the ratiometric photoluminescence response (calculated as the intensity ratio at the wavelength values indicated by the blue arrows)) and the O_2 partial pressure. Adapted with permission from Ref. [62]. Copyright 2011 Royal Society of Chemistry.

emission intensity, providing the ratiometric response. It is worth noting that in this case the ratiometric sensing stems from the inherent response of the functional ligand to oxygen and the orthogonal behaviour of the luminophores, rather than from the interaction between them.[63] QD-chromophore conjugates for the ratiometric determination of pH have also been developed.[7,48]

A more recent strategy to develop QDs-based ratiometric sensors involves the combination of two different-colour emitting nanocrystals.[64,65] In these studies, the nanohybrids are made of red-emitting CdTe QDs (rQDs), which are in turn embedded in silica nanospheres and decorated with green emitting CdTe QDs (gQDs). In this way, gQDs can become in contact with the analytes, while rQDs are isolated from it.

Following this strategy, Zhou and coworkers[64] developed a ratiometric probe for glucose in which 3-aminophenylboronic acid (APBA) was chosen as a ligand to decorate the outer gQDs (Figure 11). The detection of glucose with boronic acid-capped QDs was already tested;[66] the recognition mechanism relies on the well-known, specific covalent interactions between the hydroxy groups of the boronic acid and the two pairs of *cis*-diol moieties of glucose. The binding process mediates the aggregation of the silica nanospheres (Figure 11), which results in the quenching of the gQDs, while the embedded rQDs retain their emission intensity. Under optimized conditions, this ratiometric probe was exploited for selective detection of glucose in a concentration range from 0.1 to 2.0 mmol/L, and was also tested in human serum samples.

The design developed by Wang and coworkers[65] differs from the previous one for the outer surface-bound ligand.

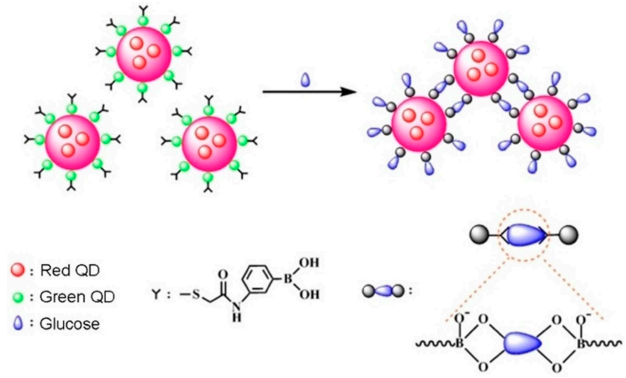

Figure 11. Schematic representation of the glucose-induced aggregation of nanohybrids containing green- and red-emitting CdTe QDs embedded in silica particles. Adapted with permission from Ref. [64]. Copyright 2016 Elsevier.

Indeed, in this work 1,10-phenanthroline (phen) was used in the place of APBA as the capping ligand for the gQDs (Figure 12). Owing to its chelating ability and affinity for cadmium atoms, phen can efficiently coordinate to the surface of the CdTe nanocrystals; moreover, a photoinduced hole transfer from the QD to phenanthroline is responsible for the luminescence quenching of the former (see B in Figure 12). The formation of not emissive ground state complexes was also reported for similar phenanthroline-decorated QDs.[67] In presence of cysteine (Cys) or homocysteine (Hcy), however, the emission intensity of gQDs could be gradually recovered (C and D in Figure 12), owing to the displacement of the phenanthroline quencher. Such a ligand exchange is afforded by the amino, thiolic and carboxylic moieties of the analytes which thus behave as multidentate competitive ligands. The detection limits of Cys and Hcy were found to be 2.5 and 1.7 μM, respectively.

It is worth mentioning that, in addition to the above discussed quantitative information, appropriately designed

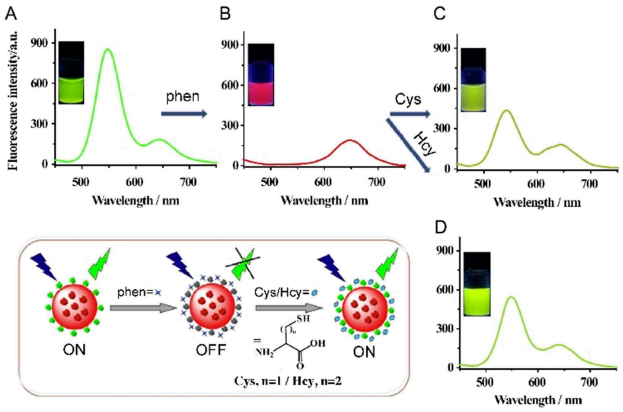

Figure 12. Fluorescence spectrum of a multicolour QD-based probe before (A) and after (B) ligand exchange with phen (aqueous buffer, λ_{exc} = 365 nm). The emission of the gQDs, initially quenched by phen, can be recovered upon addition of cysteine (C) and homocysteine (D). The box shows a schematic representation of the detection mechanism. Adapted with permission from Ref. [65]. Copyright 2015 Elsevier.

ratiometric nanoprobes can enable the determination of the presence of the analyte on site by the naked eye. This is very useful when a response is required in remote or inaccessible locations, or at the point of care in medical diagnostics.

3. QDs as Photosensitizers of Molecular Triplet Excited States

In recent years, the observation of Dexter-type triplet-triplet energy transfer from quantum dots to molecular ligands[68] has paved the way for the development of novel triplet photosensitizers based on inorganic QD-organic chromophore nanohybrids. Besides the possibility of adjusting the exciton energy level by changing the size of the nanoparticles, the main advantage of using semiconductor nanocrystals in this context arises from the closer energy spacing between the excited levels (1–15 meV)[69] compared to the large and energy-wasting singlet-triplet splitting of molecular sensitizers.

In the work of Castellano and collaborators,[68] CdSe QDs with a diameter of 2.4 nm were functionalized with 9-anthracenecarboxylic acid (9-ACA). Transient absorption spectroscopy experiments revealed that, upon selective excitation of the nanocrystals, the exciton state decays within a timescale coinciding with the rise of the T_1-T_n transitions of 9-ACA. These experiments are fully consistent with the photosensitization of the lowest triplet excited state of the anthracenyl moiety by the colloidal nanocrystals.

As previously mentioned, the energy spacing between the "bright" (i.e., singlet-like character) and "dark" (i.e., triplet-like character) exciton states of the CdSe nanocrystals is about 10 meV. It is thus reasonable to assume that the dark states, lying only a few meV below the bright states that give rise to the QD emission, are involved in the Dexter-type energy transfer from the QD to the 9-ACA ligand. Subsequent energy transfer from the excited triplet of the surface-bound chromophore to suitable energy acceptors in solution, as well as the generation of $^1O_2$, were also demonstrated.[68] It is worth noting that Dexter-type energy transfer in the reverse direction, that is, from photogenerated organic triplets to PbSe and PbS QDs, was also observed.[70]

These results clearly demonstrate that QDs are suitable candidates for triggering a range of photoprocesses relevant for practical applications, such as photon up-conversion arising from triplet-triplet annihilation.[68,71] Optical up-conversion – a process in which two or more low-energy photons are converted into a single higher-energy photon – is of interest for applications such as bioimaging, night vision, multi-dimensional displays, and photovoltaics. Specifically, in photovoltaic applications an optical up-conversion layer can capture sub-bandgap photons, increasing the efficiency of a conventional single-junction device.[71c]

Building on these findings, we hypothesized that if the exciton level of the nanocrystal is quasi-isoenergetic with the long-lived triplet state of a surface-anchored organic chromophore, QDs with novel photophysical properties could be obtained.[72] In particular, if the inter-component energy transfer in such nanoconjugates is fast with respect to other deactivation pathways, reversible (i.e., bidirectional) electronic energy transfer (REET) between chromophores may take place.[73] This process could substantially modify the photophysical behaviour of the nanocrystal, particularly with regard to its luminescence lifetime, as it has been previously observed for molecular dyads.[74] In fact, a fast REET process causes the equilibration of the QD exciton with the molecular-based excited triplet; as the latter is much longer lived than the former, it can play as a reservoir for electronic energy, and thermally activated delayed luminescence of the QD can occur. In other words, the lifetime of the QD-based emission in the nanohybrid would increase as a consequence of REET. The key advantage of using quantum dots in this context is that the exciton energy can be finely tuned by changing the diameter of the nanoparticle. Such an engineering of the energy difference between the QD and molecular levels enables a precise control of the REET phenomenon.

To verify this hypothesis, we prepared four samples of CdSe QDs with different size (diameter from 2.6 to 5.7 nm) and decorated them with 1-pyrenecarboxylic acid (PCA) (Figure 13).[75] PCA was chosen as the chromophore because of the inherent properties of its lowest triplet state ($^3\pi\pi^*$; $\tau_T \approx 10$ ms, $E_T = 2.1$ eV) and the efficient coordination of its carboxylate group to the surface of nanocrystals.[76]

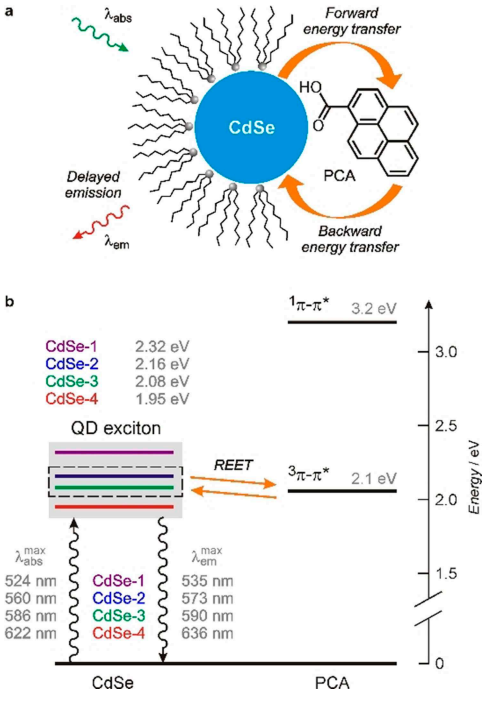

Figure 13. (a) Schematic representation of the photoinduced processes in a nanoconjugate consisting of CdSe QD and PCA components. (b) Energy-level diagram for the four different nanohybrids. Samples CdSe-2/PCA and CdSe-3/PCA can exhibit reversible electronic energy transfer (REET) involving their exciton level and the energy-matched triplet excited state of PCA. The QD exciton levels of hybrids CdSe-1/PCA and CdSe-4/PCA are too high and too low, respectively, for REET to occur at room temperature. Adapted with permission from Ref. [75]. Copyright 2018 Wiley-VCH.

Although the pyrenyl ligand did not affect either the energy or the shape of the QD emission, significant changes in the luminescence lifetime were observed for samples CdSe-2/PCA and CdSe-3/PCA. Specifically, a component in the 100-μs domain appeared in their emission decay monitored at room temperature in deoxygenated heptane (Figure 14, a and b). Such a long-lived component was not detected either in air-equilibrated solution (Figure 14c), due to the efficient quenching of the pyrene triplet by oxygen, or in case of samples of CdSe-2 and CdSe-3 QDs not functionalized with the PCA ligand. In contrast, samples CdSe-1 and CdSe-4 capped with PCA, did not show any lifetime elongation in deoxygenated solution (Figure 14d). This observation can be ascribed to the fact that in these nanohybrids the energy difference between the emitting state of the QD and the lowest triplet state of PCA is too large to allow a fast REET and lead to the thermal equilibration of the excited levels (Figure 13).

Such an approach is very interesting because it enables the preparation of QDs with the same emission maximum and bandshape but different lifetime. The versatility of the design is guaranteed by the size-dependent photophysics of QDs and the wide variety of available molecular chromophores. Nanohybrids endowed with a long-lived emission can be of high interest for time-gated applications and, potentially, add a novel dimension to multiplexed analyses.[51] Nonetheless, an unprecedented oxygen sensitivity, based on the QD emission, can be implemented within nanocrystals which are inherently O_2-insensitive.

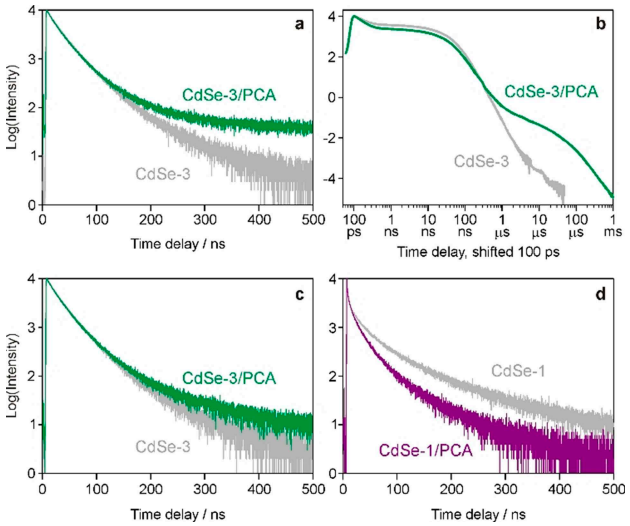

Figure 14. Luminescence decay of CdSe-3/PCA QDs monitored at 600 nm (green trace) in deoxygenated solution, as measured by (a) time-correlated single-photon counting (log plot, λ_{exc} = 405 nm) and (b) gated streak camera (log-log plot, λ_{exc} = 465 nm). (c) Luminescence decay of CdSe-3/PCA QDs (λ_{exc} = 405 nm, green trace) in air equilibrated solution. (d) Luminescence decay of CdSe-1/PCA monitored at 540 nm (λ_{exc} = 405 nm, purple trace) in deoxygenated solution. The grey traces in all panels refer to the same experiment performed on the same QD sample lacking the PCA functionalization. Conditions: heptane, room temperature. Adapted with permission from Ref. [75]. Copyright 2018 Wiley-VCH.

4. Photocatalysis

The application of colloidal semiconductor nanocrystals in photocatalysis, taking advantage of the combination of size-tunable redox and optoelectronic properties, can bring about a number of advantages with respect to traditional systems based on transition-metal oxides[77] and precious-metal coordination compounds.[78] Although a significant photooxidation of water by using quantum dots has not yet been achieved, the photoreduction half-cycle reactions afforded turnover numbers (TONs) higher than 10^5. This result can be ascribed to an efficient charge separation between the nanocrystal surface and a peripheral metal catalyst.[79]

Photocatalytic conversion of CO_2 into carbonaceous feedstock chemicals is a promising strategy to mitigate greenhouse gas emissions and simultaneously store solar energy in chemical form. Reisner and coworkers[80] employed CdS QD-based hybrid nanocatalysts in the photoconversion of CO_2 to CO, with the aim of reducing cost and environmental impact, and improving the selectivity of the process. In this work, a series of electrocatalysts for the reduction of CO_2 to CO in organic media, such as nickel-terpyridine complexes, were attached to water-soluble CdS QDs by means of different surface coordinating groups (Figure 15). This approach has several practical advantages. First, it does not require the use of precious metal catalysts or photosensitizers that are highly reactive and air sensitive, or expensive enzymes that are difficult to handle. Second, it provides a route for employing organic electrocatalysts in aqueous solutions.

Under the conditions adopted in the experiments, the first step of the CO_2 conversion process is a photoinduced electron transfer from the CdS QD to the surface-bound molecular catalyst (Figure 15). Hence, the selectivity of the overall process is strongly dependent on the nature of the anchoring groups. If the catalyst is detached from the surface, the Ni^{2+} ions released upon photodecomposition of the metal complex can cause the production of molecular hydrogen at the CdS surface, as already observed in similar systems.[81] A selectivity for CO generation higher than 90% was observed in case of the nickel-terpyridine complex bearing thiol moieties (that is, $[Ni(terpyS)_2]^{2+}$, Fig-

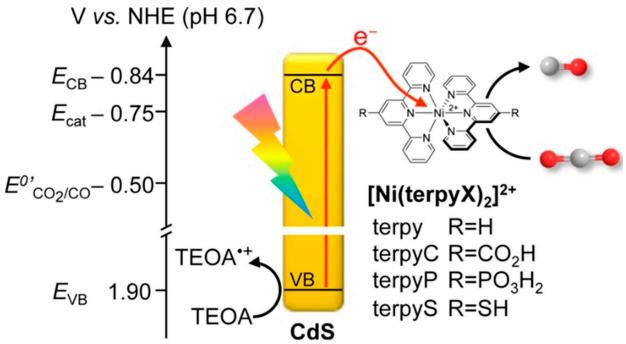

Figure 15. Schematic representation of a photocatalytic nanohybrid consisting of a molecular nickel bis(terpyridine) catalyst anchored on a CdS QD photosensitizer. The performance of different anchoring groups (R) was investigated. Reproduced with permission from Ref. [80]. Copyright 2017 American Chemical Society.

ure 15), which exhibit a strong affinity for the CdS surface. This study clearly demonstrates that the adsorption of the catalyst on the nanocrystal is a fundamental requirement to achieve selective CO_2 reduction in aqueous solution, and provides an example of a precious-metal-free photocatalytic nanohybrid.

The previously discussed ability of semiconductor nanocrystals to photosensitize molecular triplets (Section 3) offers novel opportunities for the application of QDs in light-triggered redox reactions. First, employing semiconductor nanocrystals as triplet sensitizers of coordination compounds with photoredox activity would prevent a few common drawbacks of QD-based photocatalytic materials in aqueous media, such as photocorrosion and poor colloidal stability in acidic solutions.[79] Moreover, the combination of semiconductor nanocrystals with molecular catalysts can extend the usable portion of the solar spectrum in the visible range. In most coordination compounds, triplet states are populated by intersystem crossing from the upper-lying singlet excited states generated by photoexcitation. This process is normally accompanied by a significant loss of energy (on the order of 1 eV). Such an energy loss is much less important if QDs are involved because, as mentioned in Section 3, the energy difference between the "bright" and "dark" exciton levels in colloidal nanocrystals is remarkably smaller than the excited singlet-triplet difference in molecular photosensitizers. Indeed, there is ample space for progress in the QD-sensitization of triplet excited states of photoredox coordination compounds.[79]

5. Phototherapy

Colloidal QDs with appropriately modified surfaces are interesting for applications in biomedical areas, whit a main focus on photodynamic therapy (PDT) and photoactivated drug delivery.[7d,82] A common issue of PDT is that the success of the therapy is strongly related to the concentration of oxygen in the target tissue; in fact, hypoxia can determine a poorer response on the tumour during the treatment. Such a limitation can be overcome by combining PDT with chemotherapy, that is, generating singlet oxygen together with an antitumour species.[83] In this regard, a good candidate as a therapeutic agent is nitric oxide (NO).

NO is an endogenously produced biological signalling molecule whose role in processes related to the immune response, smooth muscle vascular tone control, neuronal communication, gene regulation, and cancer biology is now well established.[84] The development of platforms that can specifically target cancer cells and control the delivery of suitable amounts of NO is indeed promising for advances in cancer therapy.[85] Photoactive colloidal nanocrystals are promising candidates in this context for combining the delivery of NO in specific district of the body and its photocontrolled release at a given time.[86,87] QD-based nanohybrids can be engineered in order to behave as supramolecular light-harvesting antennas in the optical therapeutic window (that is, 650–900 nm), thus affording the release of NO from suitable surface-bound ligands.

The first study on the photosensitized release of NO mediated by colloidal nanocrystals was reported by Ford and colleagues.[88] In this work, a cationic metal complex such as *trans*-Cr^{III}(cyclam)$(ONO)_2^+$ (CrONO in Figure 16) was investigated as a photocaged NO ligand, in combination with anionic water-soluble CdSe–ZnS core-shell QDs. The electrostatic adsorption of CrONO on the negatively charged dihydrolipoate capping ligands (Figure 16a) enables FRET from the nanocrystal to the chromium complex and causes the photocleavage of the CrO–NO bond, thus affording NO plus a *trans*-Cr^{IV}O(cyclam)$(ONO)^+$ intermediate species. The mechanism involves the photosensitization of the quartet excited state of the metal complex (^{4}CrONO* in Figure 16b) by the CdSe–ZnS QDs, followed by a fast intersystem crossing that populates a reactive doublet excited state (^{2}CrONO*), which ultimately releases NO.

In a successive study, the photorelease of NO was optimized by modifying the macrocycle that coordinates the metal ion and the related counter anion, as well as by adapting the size and composition of the QD to improve the FRET efficiency.[89]

Among the many different compounds investigated as potential NO donors in vivo, ruthenium nitrosyls (Ru–NO) exhibit unique properties such as low cytotoxicity and good stability under various biological conditions. Ford, da Silva and coworkers[82] employed water-soluble CdTe QDs passivated by mercaptopropionic acid to photosensitize the ruthenium nitrosyl complex *cis*-$[Ru(NO)(4\text{-ampy})(bpy)_2]^{3+}$ (bpy = 2,2′-bipyridine, 4-ampy = 4-aminopyridine) and promote NO release. Because of the lack of overlap between the QD-based emission and the

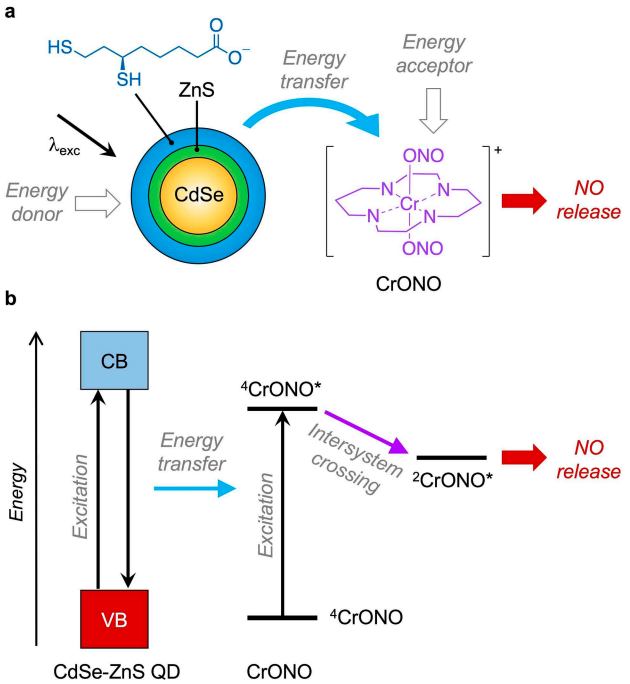

Figure 16. Schematic representation (a) and energy-level diagram describing the photoinduced release of NO in CdSe–ZnS nanocrystals assembled with a chromium complex. Excitation of the QDs coated with dihydrolipoate ligands is followed by energy transfer to the CrONO complex, adsorbed on the nanocrystal surface, and release of NO. Adapted with permission from Ref. [86]. Copyright 2016 Springer-Verlag.

Ru–NO absorption bands, FRET is unlikely to contribute to the release mechanism, which was rationalized in terms of charge transfer from the excited CdTe core to the adsorbed ruthenium complex. The efficiency of the overall process was found to be 8-fold higher than that observed in the bare Ru–NO complex. A related system with similar NO donors was recently developed using N-doped graphene QDs equipped with a liver-targeting galactose derivative for the recognition of liver cancer cells.[90] Nanohybrids based on CdSe or CdSe–ZnS QDs were also tested for combining together luminescence imaging and the release of the well-known antitumor drug cisplatin.[91]

In order to address essential requirements for medical applications, such as deeper tissue penetration and biocompatibility, novel cadmium-free QDs that can absorb near infrared light,[92] such as $CuInS_2$-ZnS,[93] are being actively investigated as novel theranostic nanomaterials. [94]

6. Conclusions

The cadmium chalcogenides have endured as the prototypical quantum dots because of their excellent spectroscopic and electronic properties. Thanks to their versatile surface functionalization, these QDs have emerged as outstanding scaffolds for the construction of multicomponent nanocrystal-molecule hybrids capable of performing useful light-induced functions. The fact that QD-molecule nanohybrids can take part in supramolecular phenomena such as inter-component energy and electron transfer, ion and molecular recognition, self-assembly and aggregation forms the basis for the development of novel nanomaterials that can find applications in analytical sciences, catalysis, materials science, energy conversion and storage, and medical therapies.

Recent research featuring these materials, such as that described here, has resulted in improved optical sensing capabilities, photosensitization of both catalysis and drug delivery and, especially, sets the scene for a future where QDs will be exploited to their fullest. On the other hand, the broad field of supramolecular systems and materials can take great benefit from the use of nanocrystals as building blocks with made-to-order photophysical properties.

Acknowledgements

Financial support from the EU (ERC AdG n. 692981), Ministero dell'Istruzione, Università e Ricerca (FARE Grant n. R16S9XXKX3), Università di Bologna and Consiglio Nazionale delle Ricerche is gratefully acknowledged.

Keywords: quantum dots · triplet sensitization · sensing · catalysis · supramolecular chemistry

[1] A. P. Alivisatos, *J. Phys. Chem.* **1996**, *100*, 13226–13239.
[2] U. Resch-Genger, M. Grabolle, S. Cavaliere-Jaricot, R. Nitschke, T. Nann, *Nat. Methods* **2008**, *5*, 763–775.
[3] A. I. Ekimov, Al. L. Efros, A. A. Onushchenko, *Solid State Commun.* **1985**, *56*, 921–924.
[4] L. E. Brus, *J. Chem. Phys.* **1984**, *80*, 4403–4409.
[5] See, e.g.: C. B. Murray, D. J. Norris, M. G. Bawendi, *J. Am. Chem. Soc.* **1993**, *115*, 8706–8715.
[6] More than 15000 articles published in the period 1999–2018; from less than 150 articles in 1999 to more than 1600 in 2018. Web of Science, November 2019; search term: "luminescen* quantum dot*" as topic.
[7] See, e.g.:a) R. C. Somers, M. G. Bawendi, D. G. Nocera, *Chem. Soc. Rev.* **2007**, *36*, 579–591; b) D. V. Talapin, J. S. Lee, M. V. Kovalenko, E. V. Shevchenko, *Chem. Rev.* **2010**, *110*, 389–458; c) C. de Mello Donega, *Chem. Soc. Rev.* **2011**, *40*, 1512–1546; d) T. L. Doane, C. Burda, *Chem. Soc. Rev.* **2012**, *41*, 2885–2911; e) M. Amelia, C. Lincheneau, S. Silvi, A. Credi, *Chem. Soc. Rev.* **2012**, *41*, 5728–5743; f) Y. Shirasaki, G. J. Supran, M. G. Bawendi, V. Bulovic, *Nat. Photonics* **2013**, *7*, 13–23; g) P. Reiss, M. Carriere, C. Lincheneau, L. Vaure, S. Tamang, *Chem. Rev.* **2016**, *116*, 10731–10819.
[8] See, e.g.:a) *Nanoparticles: from theory to applications* (Ed.: G. Schmid), Wiley-VCH, Weinheim, **2004**; b) *Semiconductor and metal nanocrystals* (Ed.: V. I: Klimov), Dekker, New York, **2005**; c) *Semiconductor nanocrystal quantum dots* (Ed.: A. L. Rogach), Springer, Vienna, **2008**; d) *Quantum dot sensors: technology and commercial applications* (Eds.: J. F. Callan, F. M. Raymo), Pan Stanford Publishing, Singapore, **2013**; e) *Photoactive Semiconductor Nanocrystal Quantum Dots – Fundamentals and Applications* (Ed.: A. Credi), Springer, Basel, **2016**.
[9] a) M. J. Fernée, P. Tamarat, B. Lounis, *Chem. Soc. Rev.* **2014**, *43*, 1311–1337; b) J. M. Pietryga, Y.-S. Park, J. Lim, A. F. Fidler, W. K. Bae, S. Brovelli, V. I. Klimov, *Chem. Rev.* **2016**, *116*, 10513–10622.
[10] a) X. Dai, Y. Deng, X. Peng, Y. Jin, *Adv. Mater.* **2017**, *29*, 1607022; b) H. Chen, J. He, S. Wu, *IEEE J. Sel. Top. Quantum Electron.* **2017**, *23*, 1900611.
[11] a) M. A. Boles, D. Ling, T. Hyeon, D. V. Talapin, *Nat. Mater.* **2016**, *15*, 141–153; b) J. Owen, L. Brus, *J. Am. Chem. Soc.* **2017**, *139*, 10939–10943; c) M. J. Smith, C. H. Lin, S. Yu, V. V. Tsukruk, *Adv. Opt. Mater.* **2019**, *7*, 1801072.
[12] a) A. Credi, *J. New. Chem.* **2012**, *36*, 1925–1930; b) J. Pérez-Prieto, *Photochem. Photobiol.* **2013**, *89*, 1291–1298; c) T. Avellini, C. Lincheneau, F. Vera, S. Silvi, A. Credi, *Coord. Chem. Rev.* **2014**, *263–264*, 151–160.
[13] R. D. Harris, S. Bettis Homan, M. Kodaimati, C. He, A. B. Nepomnyashchii, N. K. Swenson, S. Lian R Calzada, E. A. Weiss, *Chem. Rev.* **2016**, *116*, 12865–12919.
[14] Q. A. Akkerman, G. Rainò, M. V. Kovalenko, L. Manna, *Nat. Mater.* **2018**, *17*, 394–405.
[15] See, e.g.:a) A. Swarnkar, A. R. Marshall, E. M. Sanehira, B. D. Chernomordik, D. T. Moore, J. A. Christians, T. Chakrabarti, J. M. Luther, *Science* **2016**, *354*, 92–95; b) F. Liu, Y. Zhang, C. Ding, S. Kobayashi, T. Izuishi, N. Nakazawa, T. Toyoda, T. Ohta, S. Hayase, T. Minemoto, K. Yoshino, S. Dai, Q. Shen, *ACS Nano* **2017**, *11*, 10373–10383.
[16] a) K. E. Knowles, K. H. Hartstein, T. B. Kilburn, A. Marchioro, H. D. Nelson, P. J. Whitham, D. R. Gamelin, *Chem. Rev.* **2016**, *116*, 10820–10851; b) W. van der Stam, A. C. Berends, C. D. Donega, *ChemPhysChem* **2016**, *17*, 559–581; c) Y.-H. Won, O. Cho, T. Kim, D.-Y. Chung, T. Kim, H. Chung, H. Jang, J. Lee, D. Kim, E. Jang, *Nature* **2019**, *575*, 634–638.
[17] L. Ye, K.-T. Yong, L. Liu, I. Roy, R. Hu, J. Zhu, H. Cai, W.-C. Law, J. Liu, K. Wang, J. Liu, Y. Liu, Y. Hu, X. Zhang, M. T. Swihart, P. N. Prasad, *Nat. Nanotechnol.* **2012**, *7*, 453–458.
[18] a) M. Bottrill, M. Green, *Chem. Commun.* **2011**, *47*, 7039–7050; b) K.-T. Yong, W.-C. Law, R. Hu, L. Ye, L. Liu, M. T. Swihart, P. N. Prasad, *Chem. Soc. Rev.* **2013**, *42*, 1236–1250.
[19] A. I. Ekimov, F. Hache, M. C. Schanne-Klein, D. Ricard, C. Flytzanis, I. A. Kudryavtsev, T. V. Yazeva, A. V. Rodina, Al. L. Efros, *J. Opt. Soc. Am. B* **1993**, *10*, 100–107.
[20] W. W. Yu, L. Qu, W. Guo, X. Peng, *Chem. Mater.* **2003**, *15*, 2854–2860.
[21] Y. Zhou, H. Zhao, D. Ma, F. Rosei, *Chem. Soc. Rev.* **2018**, *47*, 5866–5890.
[22] Y. Shen, M. Y. Gee, A. B. Greytak, *Chem. Commun.* **2017**, *53*, 827–841.
[23] R. Bilan, F. Fleury, I. Nabiev, A. Sukfhanova, *Bioconjugate Chem.* **2015**, *26*, 609–624.
[24] J. Hu, Z.-Y Wang, C.-C Li, C.-Y Zhang, *Chem. Commun.* **2017**, *53*, 13284–13295.
[25] a) M. A. H. Hines, P. Guyot-Sionnest, *J. Phys. Chem.* **1996**, *100*, 468–471; b) J. J. Li, Y. A Wang, W. Guo, J. C. Keay, T. D. Mishima, M. B. Johnson, X. Peng, *J. Am. Chem. Soc.* **2003**, *125*, 12567–12575.
[26] a) P. Reiss, M. Protière, L. Li, *Small* **2009**, *5*, 154–168; b) R. G. Chaudhuri, S. Paria, *Chem. Rev.* **2012**, *112*, 2373–2433.

[27] a) S. J. Lim, L. Ma, A. Schleife, A. M. Smith, *Coord. Chem. Rev.* **2016**, *320*, 216–237; b) S. V. Kilina, P. K. Tamukong, D. S. Kilin, *Acc. Chem. Res.* **2016**, *49*, 2127–2135.
[28] M. L. H. Green, *J. Organomet. Chem.* **1995**, *500*, 127–148.
[29] a) M. L. H. Green, G. Parkin, *J. Chem. Educ.* **2014**, *91*, 807–816; b) J. Owen, *Science* **2015**, *347*, 615–616.
[30] C. Giansante, I. Infante, *J. Phys. Chem. Lett.* **2018**, *8*, 5209–5215.
[31] a) G. Kalyuzhny, R. W. Murray, *J. Phys. Chem. B* **2005**, *109*, 7012–7021; b) C. Bullen, P. Mulvaney, *Langmuir* **2006**, *22*, 3007–3013.
[32] A. H. Ip, S. M. Thon, S. Hoogland, O. Voznyy, D. Zhitomirsky, R. Debnath, L. Levina, L. R. Rollny, G. H. Carey, A. Fischer, K. W. Kemp, I. J. Kramer, Z. Ning, A. J. Labelle, K. W. Chou, A. Amassian, E. H. Sargent, *Nat. Nanotechnol.* **2012**, *7*, 577–582.
[33] V. Arora, U. Soni, M. Mittal, S. Yadav, S. Sapra, *J. Colloid Interface Sci.* **2017**, *491*, 329–335.
[34] N. Kirkwood, J. O. V. Monchen, R. W. Crisp, G. Grimaldi, H. A. C. Bergstein, I. du Fossé, W. van der Stam, I. Infante, A. J. Houtepen, *J. Am. Chem. Soc.* **2018**, *140*, 15712–15723.
[35] a) V. Lesnyak, N. Gaponik, A. Eychmüller, *Chem. Soc. Rev.* **2013**, *42*, 2905–2929; b) Y. Pu, F. Cai, D. Wang, J.-X. Wang, J.-F. Chen, *Ind. Eng. Chem. Res.* **2018**, *57*, 1790–1802.
[36] a) M. Green, *J. Mater. Chem.* **2010**, *20*, 5797–5809; b) A. J. Morris-Cohen, M. Malicki, M. D. Peterson, J. W. J. Slavin, E. A. Weiss, *Chem. Mater.* **2013**, *25*, 1155–1165.
[37] See, e.g.:a) H. T. Uyeda, I. L. Medintz, J. K. Jaiswal, S. M. Simon, H. Mattoussi, *J. Am. Chem. Soc.* **2005**, *127*, 3870–3878; b) Z. Popovic, W. Liu, W. P. Chauhan, J. Lee, C. Wong, A. B. Greytak, N. Insin, D. G. Nocera, D. Fukumura, R. K. Jain, M. G. Bawendi, *Angew. Chem. Int. Ed.* **2010**, *49*, 8649–8652; *Angew. Chem.* **2010**, *122*, 8831–8834; c) C. Giansante, *Nanoscale* **2019**, *11*, 9478–9487.
[38] See, e.g.:a) I. Yildiz, E. Deniz, B. McCaughan, S. F. Cruickshank, J. F. Callan, F. M. Raymo, *Langmuir* **2010**, *26*, 11503–11511; b) N. Zhan, G. Palui, J.-P. Merkl, H. Mattoussi, *J. Am. Chem. Soc.* **2016**, *138*, 3190–3201.
[39] a) T. Avellini, C. Lincheneau, M. La Rosa, A. Pertegás, H. J. Bolink, I. A. Wright, E. C. Constable, S. Silvi, A. Credi, *Chem. Commun.* **2014**, *50*, 11020–11022; b) M. La Rosa, T. Avellini, C. Lincheneau, S. Silvi, I. A. Wright, E. C. Constable, A. Credi, *Eur. J. Inorg. Chem.* **2017**, *44*, 5143–5151.
[40] a) G. Palui, T. Avellini, N. Zhan, F. Pan, D. Gray, I. Alabugin, H. Mattoussi, *J. Am. Chem. Soc.* **2012**, *134*, 16370–16378; b) F. Aldeek, D. Hawkins, V. Palomo, M. Safi, G. Palui, P. E. Dawson, I. Alabugin, H. Mattoussi, *J. Am. Chem. Soc.* **2015**, *137*, 2704–2714.
[41] See, e.g.:a) B. Dubertret, P. Skourides, D. J. Norris, V. Noireaux, A. H. Brivanlou, A. Libchaber, *Science* **2002**, *298*, 1759–1762; b) H. Fan, E. W. Leve, C. Scullin, J. Gabaldon, D. Tallant, S. Bunge, T. Boyle, M. C. Wilson, C. J. Brinker, *Nano Lett.* **2005**, *5*, 645–648; c) A. M. Smith, H. Duan, M. N. Rhyner, G. Ruan, S. Nie, *Phys. Chem. Chem. Phys.* **2006**, *8*, 3895–3903.
[42] See, e.g.:a) J. Li, X. Li, R. Yang, L. Qu, P. de B Harrington, *Anal. Chim. Acta* **2013**, *804*, 76–83; b) J. Lee, C.-S. Han, *Nanoscale Res. Lett.* **2015**, *10*, 145.
[43] See, e.g.:a) T. Pellegrino, L. Manna, S. Kudera, T. Liedl, D. Koktysh, A. L. Rogach, S. Keller, J. Rädler, G. Natile, W. J. Parak, *Nano Lett.* **2004**, *4*, 703–707; b) W. W. Yu, E. Chang, J. C. Falkner, J. Zhang, A. M. Al-Somali, C. M. Sayes, J. Johns, R. Drezek, V. L. Colvin, *J. Am. Chem. Soc.* **2007**, *129*, 2871–2879; c) E. Peng, E. S. G. Choo, C. S. H. Tan, X. Tang, Y. Sheng, J. Xue, *Nanoscale* **2013**, *5*, 5994–6005.
[44] See, e.g.: C.-Y. Chen, C.-T. Cheng, C.-W. Lai, P.-W. Wu, K.-C. Wu, P.-T. Chou, Y.-H. Chou, H.-T. Chiu, *Chem. Commun.* **2006**, 263–265.
[45] See, e.g.: J. Aguilera-Sigalat, J. M. Casas-Solvas, M. C. Morant-Miñana, V. Vargas-Berenguel, R. E. Galian, J. Pérez-Prieto, *Chem. Commun.* **2012**, *48*, 2573–2575.
[46] H. J. Kim, M. H. Lee, L. Mutihac, J. Vicens, J. S. Kim, *Chem. Soc. Rev.* **2012**, *41*, 1173–1190.
[47] S.-C. Cui, T. Tachikawa, M. Fujitsuka, T. Majima, *J. Phys. Chem. C* **2011**, *115*, 1824–1830.
[48] a) J. F. Callan, A. P. De Silva, R. C. Mulrooney, B. Mc Caughan, *J. Inclusion Phenom. Macrocyclic Chem.* **2007**, *58*, 257–262; b) F. M. Raymo, I. Yildiz, *Phys. Chem. Chem. Phys.* **2007**, *9*, 2036–2043; c) R. Freeman, I. Willner, *Chem. Soc. Rev.* **2012**, *41*, 4067–4085; d) S. Silvi, A. Credi, *Chem. Soc. Rev.* **2015**, *44*, 4275–4289; e) I. V. Martynenko, A. P. Litvin, F. Purcell-Milton, A. V. Baranov, A. V. Fedorov, Y. K. Gun'ko, *J. Mater. Chem. B* **2017**, *5*, 6701–6727.
[49] a) V. Balzani, A. Credi, M. Venturi, *Molecular devices and machines-Concepts and perspectives for the nanoworld*, Wiley-VCH, Germany, **2008**; b) J. R. Lakowicz, *Principles of fluorescence spectroscopy, 3rd Ed.*, Springer, New York, **2006**.
[50] a) A. Clapp, I. L. Medintz, H. Mattoussi, *ChemPhysChem* **2006**, *7*, 47–57; b) I. Yildiz, M. Tomasulo, F. M. Raymo, *J. Mater. Chem.* **2008**, *18*, 5577–5584.
[51] N. Hildebrandt, C. M. Spillmann, W. R. Algar, T. Pons, M. H. Stewart, E. Oh, K. Susumu, S. A. Díaz, J. B. Delehanty, I. L. Medintz, *Chem. Rev.* **2017**, *117*, 536–711.
[52] J. Völker, X. Zhou, X. Ma, S. Flessau, H. Lin, M. Schmittel, A. Mews, *Angew. Chem. Int. Ed.* **2010**, *49*, 6865–6868; *Angew. Chem.* **2010**, *122*, 7017–7020.
[53] Y. Lou, Y. Zhao, J. Chena, J.-J. Zhu, *J. Mater. Chem. C* **2014**, *2*, 595–613.
[54] J. Pei, H. Zhu, X. Wang, H. Zhang, X. Yang, *Anal. Chim. Acta* **2012**, *757*, 63–68.
[55] Y. F. Chen, Z. Rosenzweig, *Anal. Chem.* **2002**, *74*. 5132–5138.
[56] R. K. Sajwan, Y. Bagbi, P. Sharma, P. R. Solanki, *J. Lumin.* **2017**, *187*, 126–132.
[57] H. Elmizadeh, M. Soleimani, F. Faribod, G. R. Bardajee, *J. Fluoresc.* **2017**, *27*, 2323–2333.
[58] C. Boonme, T. Noipa, T. Tuntulani, W. Ngeontae, *Spectrochim. Acta. A Mol. Biomol. Spectrosc.* **2013**, *169*, 161–168.
[59] N. Mahapatra, A. Mandal, S. Panja, M. Halder, *Sens. Actuators B* **2017**, *240*, 543–552.
[60] T. Fang, K. G. Ma, L. L. Ma, J. Y. Bai, X. Li, H. H. Song, H. Q. Guo, *J. Phys. Chem. C* **2012**, *116*, 12346–12352.
[61] a) A. Mandal, A. Dandapat, G. De, *Analyst* **2012**, *137*, 765–772; b) Y. S. Xia, C. Cao, C. Q. Zhu, *J. Lumin.* **2008**, *128*, 166–172; c) T. T. Gan, Y. J. Zhang, N. J. Zhao, X. Xiao, G. F. Yin, S. H. Yu, H. B. Wang, J. B. Duan, C. Y. Shi, W. Q. Liu, *Spectrochim. Acta. A Mol. Biomol. Spectrosc.* **2012**, *99*, 62–68.
[62] M. Amelia, A. Lavie-Cambot, N. D. McClenaghan, A. Credi, *Chem. Commun.* **2011**, *47*, 325–327.
[63] S. Gonzalez-Carrero, M. de la Guardia, R. E. Galian, J. Pérez-Prieto, *ChemistryOpen* **2014**, *3*, 199–205.
[64] T. Hao, X. Wei, Y. Nie, Y. Xu, K. Lu, Y. Yan, Z. Zhou, *Sens. Actuators B* **2016**, *230*, 70–76.
[65] K. Wang, J. Qian, D. Jiang, Z. Yang, Z. Du, K. Wang, *Biosens. Bioelectron.* **2015**, *65*, 83–90.
[66] D. B. Cordes, S. Gamsey, B. Singaram, *Angew. Chem. Int. Ed.* **2006**, *45*, 3829–3832; *Angew. Chem.* **2006**, *118*, 3913–3916.
[67] a) T. Chen, Y. Hu, Y. Cen, X. Chu, Y. Lu, *J. Am. Chem. Soc.* **2013**, *135*, 11595–11602; b) X. Hu, K. Zhu, Q. Guo, Y. Liu, M. Ye, Q. Sun, *Anal. Chim. Acta* **2014**, *812*, 191–198.
[68] C. Mongin, S. Garakyaraghi, N. Razgoniaeva, M. Zamkov, F. N. Castellano, *Science* **2016**, *351*, 369–372.
[69] G. D. Scholes, *Adv. Funct. Mater.* **2014**, *13*, 1039–1043.
[70] a) M. Tabachnyk, B. Ehrler, S. Gélinas, M. L. Böhm, B. J. Walker, K. P. Musselman, N. C. Greenham, R. H. Friend, A. Rao, *A. Nat. Mater.* **2014**, *13*, 1033–1038; b) N. J. Thompson, M. W. B. Wilson, D. N. Congreve, P. R. Brown, J. M. Scherer, T. S. Bischof, M. Wu, N. Geva, M. Welborn, T. Voorhis, V. Bulović, M. G. Bawendi, M. A. Baldo, *Nat. Mater.* **2014**, *13*, 1039–1043.
[71] a) Z. Huang, X. Li, M. Mahboub, K. M. Hanson, V. M. Nichols, H. Le, M. L. Tang, C. J. Bardeen, *Nano Lett.* **2015**, *15*, 5552–5557; b) Z. Huang, X. Li, B. D. Yip, J. M. Rubalcava, C. J. Bardeen, M. L. Tang, *Chem. Mater.* **2015**, *27*, 7503–7507; c) M. Wu, D. N. Congreve, M. W. B. Wilson, J. Jean, N. Geva, M. Welborn, T. Van Voorhis, V. Bulović, M. G. Bawendi, M. A. Baldo, *Nat. Photonics* **2016**, *10*, 31–34.
[72] M. Baroncini, M. Canton, L. Casimiro, S. Corra, J. Groppi, M. La Rosa, S. Silvi, A. Credi, *Eur. J. Inorg. Chem.* **2018**, *42*, 4589–4603.
[73] A. Lavie-Cambot, C. Lincheneau, M. Cantuel, Y. Leydet, N. D. McClenaghan, *Chem. Soc. Rev.* **2010**, *39*, 506–515.
[74] See, e.g.:a) W. E. Ford, M. A. J. Rodgers, *J. Phys. Chem.* **1992**, *96*, 2917–2920; b) R. Passalacqua, F. Loiseau, S. Campagna, Y.-Q. Fang, G. S. Hanan, *Angew. Chem. Int. Ed.* **2003**, *42*, 1608–1611; *Angew. Chem.* **2003**, *115*, 1646–1649; c) G. Ragazzon, P. Verwilst, S. A. Denisov, A. Credi, G. Jonusauskas, N. D. McClenaghan, *Chem. Commun.* **2013**, *49*, 9110–9112; d) C. E. McCusker, A. Chakraborty, F. N. Castellano, *J. Phys. Chem. A* **2014**, *118*, 10391–10399.
[75] M. La Rosa, S. A. Denisov, G. Jonusauskas, N. D. McClenaghan, A. Credi, *Angew. Chem. Int. Ed.* **2018**, *57*, 3104–3107; *Angew. Chem.* **2018**, *130*, 3158–3161.
[76] Similar results were obtained independently by another research group: C. Mongin, P. Moroz, M. Zamkov, F. N. Castellano, *Nat. Chem.* **2018**, *10*, 225–230.
[77] D. M. Schultz, T. P. Yoon, *Science* **2014**, *343*, 1239176.

[78] J. J. Concepcion, J. W. Jurss, M. Kyle Brennaman, P. G. Hoertz, A. O. T. Patrocinio, N. Y. M. Iha, J. L. Templeton, T. J. Meyer, *Acc. Chem. Res.* **2009**, *42*, 121, 954–1965.
[79] P. Moroz, A. Boddy, M. Zamkov, *Front. Chem.* **2018**, *6*, 353–360.
[80] M. F. Kuehnel, K. L. Orchard, K. E. Dalle, E. Reisner, *J. Am. Chem. Soc.* **2017**, *139*, 7217–7223.
[81] a) J.-J. Wang, Z.-J. Li, X.-B. Li, X.-B. Fan, Q.-Y. Meng, S. Yu, C.-B. Li, J.-X. Li, C.-H. Tung, L.-Z. Wu, *ChemSusChem* **2014**, *7*, 1468–1475; b) Z.-J. Li, X.-B. Fan, X.-B. Li, J.-X. Li, C. Ye, J.-J. Wang, S. Yu, C.-B. Li, Y.-J. Gao, Q.-Y. Meng, C.-H Tung, L.-Z. Wu, *J. Am. Chem. Soc.* **2014**, *136*, 8261–8268; c) Z. Han, F. Qiu, R. Eisenberg, P. L. Holland, T. D. Krauss, *Science* **2012**, *338*, 1321–1324.
[82] L. P. Franco, S. A. Cicillini, J. C. Biazzotto, M. A. Schiavon, A. Mikhailovsky, P. Burks, J. Garcia, P. C. Ford, R. Santana da Silva, *J. Phys. Chem. A* **2014**, *118*, 12184–12191 and references therein.
[83] Z. A. Carneiro, J. C. Biazzotto de Moraes, F. Postalli Rodrigues, R. Galvão de Lima, C. Curti, Z. Novaes da Rocha, M. Paulo, L. M. Bendhack, A. C. Tedesco, A. L. Barboza Formiga, R. Santana da Silva, *J. Inorg. Biochem.* **2011**, *105*, 1035–1043.
[84] P. Pacher, J. S. Beckman, L. Liaudet, *Physiol. Rev.* **2007**, *87*, 315–424.
[85] A. B. Seabra, N. Duran, *J. Mater. Chem.* **2010**, *20*, 1624–1637.
[86] L. Sansalone, S. Tang, Y. Zhang, E. R. Thapaliya, F. M. Raymo, J. Garcia-Amorós, in *Photoactive Semiconductor Nanocrystal Quantum Dots-Fundamentals and Applications* (Ed.: A. Credi), Springer, Basel, **2016**, pp. 31–60.
[87] P. C. Ford, *Nitric Oxide* **2013**, *34*, 56–64.
[88] D. Neuman, A. D. Ostrowski, R. O. Absalonson, G. F. Strouse, P. C. Ford, *J. Am. Chem. Soc.* **2007**, *129*, 4146–4147.
[89] P. T. Burks, A. D. Ostrowski, A. A. Mikhailovsky, E. M. Chan, P. S. Wagenknecht, P. C. Ford, *J. Am. Chem. Soc.* **2012**, *134*, 13266–13275.
[90] Y.-H. Li, M. Guo, S.-W. Shi, Q.-L. Zhang, S.-P. Yang, J.-G. Liu, *J. Mater. Chem. B* **2017**, *5*, 7831–7838 and references therein.
[91] L.-W. Zhang, C.-J. Wen, S. A. Al-Suwayeh, T.-C. Yen, J.-Y. Fang, *J. Nanopart. Res.* **2012**, *14*, 882.
[92] P. Zhao, Q. Xu, J. Tao, Z. Jin, Y. Pan, C. Yu, Z. Yu, *WIREs Nanomed. Nanobiotechnol.* **2018**, *10*, e1483.
[93] W. Zhang, Q. Lou, W. Ji, J. Zhao, X. Zhong, *Chem. Mater.* **2013**, *26*, 1204–1212.
[94] G. Lv, W. Guo, W. Zhang, T. Zhang, S. Li, S. Chen, A. S. Eltahan, D. Wang, Y. Wang, J. Zhang, P. C. Wang, J. Chang, X.-J. Liang, *ACS Nano* **2016**, *10*, 9637–9645.

Manuscript received: November 13, 2019
Revised manuscript received: January 8, 2020